Simulation of Impurity Behaviour for Basic ITER Scenarios.

V.M.Leonov, V.E.Zhogolev

NFI, RRC « Kurchatov Institute », Moscow, Russia. e-mail: leo@nfi.kiae.ru

Abstract. Simulations of radial profiles of density and radiation of the various impurities in the basic ITER scenarios have been performed. Modeling of the initial stage of discharges with beryllium and tungsten limiters has been done. Results of calculations of power flux through the plasma boundary, plasma radiation and plasma contamination by impurities on this stage are presented. Critical concentrations of different impurities expected in ITER plasma are calculated. It was shown, that for considered ITER scenarios effective radiation from the plasma periphery is possible without the excessive accumulation of heavy impurities in the plasma core. Simulations have not demonstrated significant drawbacks in usage of high-Z materials (tungsten for example) for the plasma facing components in ITER.

1. Introduction

Plasma-surface interaction is one of the key issues in the development of the ITER design. On the one hand it is necessary to avoid impurity accumulation in the plasma core to prevent radiation losses from this region and fuel dilution. On the other hand impurity radiation from the plasma periphery helps to control power flux to the divertor preventing the overheating of the divertor plates. In this study the simulation of radial profiles of density and radiation of the impurities in the basic ITER scenarios was performed aimed, firstly, to analyze the possibility to create the re-radiating layer near the plasma boundary without impurity accumulation in the plasma core and, secondly, to estimate the critical (maximal possible) concentrations of the various impurities in the reference ITER scenario. Also, the possibility of using high-Z elements as tungsten and argon in ITER has been examined.

Modeling of impurity behaviour was performed by the ZIMPUR code [1] simulating the transport, dynamics of the charge states and radiation of impurities. Dynamics of the concentrations of impurity ions, n_k, in various charge states k, ($0 \le k \le Z$) is described by the set of equations:

$$\frac{\partial (V' n_k)}{\partial t} + \frac{\partial}{\partial \rho}\left[V' < (\nabla \rho)^2 > \Gamma_k \right] = V' n_e \left\{ I_{k-1} n_{k-1} - \left(I_k + R_k \right) n_k + R_{k+1} n_{k+1} \right\}, \quad (1)$$

where ρ is the radial coordinate, $V(\rho)$ is the volume inside the magnetic surface, Γ_k are the radial fluxes of particles, I_k is ionization rate, and R_k consists of the sum of radiation and dielectronic recombination rates, which is enlarged on the value $R_k^{cx} = <\sigma V>_k^{cx} n^0/n_e$ describing the charge exchange of impurity ions with hydrogen isotope atoms. The radiation of each sort of impurity is determined by the summation over all possible charge states, $P_Z = \Sigma L_k n_k$, where coefficients L_k include bremstrahlung, linear and recombination radiations.

For the self-consistent simulations of the ITER scenarios this code has been integrated into the ASTRA transport code [2] describing the dynamics of the background plasma parameters. For the calculation of the neoclassical impurity fluxes Γ_k^{nc} the NCLASS code [3] was used. It allows to calculate particle fluxes for the arbitrary aspect ratio and the arbitrary collisionality. Radial components of the ion impurity fluxes averaged over the magnetic surfaces include anomalous and neoclassical parts:

$$\Gamma_k = V_A n_k - D_A \partial n_k / \partial \rho + \Gamma_k^{nc}, \quad (2)$$

In this work anomalous drift velocity V_A and a diffusion coefficient D_A have been taken the same, as for the main plasma. The relations between impurity ion fluxes Γ_k^x and ion densities n_k^x at the plasma surface $\rho_n=\rho/\rho_{max}=1$ were used as the boundary conditions, $\Gamma_k^x=V_\perp n_k^x$. The value $V_\perp$ was taken to be equal to the velocity of the plasma electrons escaping the plasma column. The impurity source was defined as the impurity neutral flux on the plasma boundary (in diffusive approximation). The amplitude of this source was fitted to provide the desirable impurity contamination in plasma. For example, argon influx was set on the level providing the specified total radiated power from the plasma column (close to the design requirement [4]) restricting the power flux to the divertor at a level not exceeding 30 MW which corresponds to the power flux through the separatrix smaller than 100 MW. It gives less than 5 MW/m^2 heat load on the divertor plates which is admissible [4]. Beryllium content was chosen on the level ~ 2 % [4]. The thermalized helium pumping speed at the plasma boundary was fitted to provide $\tau_{He} / \tau_E = 3$. The bulk plasma ion density was determined from a quasi-neutrality condition taking into account all impurities, helium and 50/50 % mixture of deuterium/tritium ions .

It was supposed, that all plasma components had the same anomalous transport coefficients $D_e^{an}= D_A= \chi_e^{an}$, $\chi_i^{an} =2\chi_e^{an}$, where $\chi_e^{an} = \kappa_{an}*(1+3\cdot\rho_n^2)$. The normalization coefficient κ_{an} was fitted to obtain correspondence of the global energy confinement time to the ITER scalings [5] (in the Ohmic phase to the OH scaling, in the L-mode phase to the L-mode scaling and in the H-mode phase to the H-mode IPB98(y,2) scaling). For scenarios with the enhanced confinement this coefficient was higher than 1. In the region of the H-mode external transport barrier and ITB region, transport coefficients of the main plasma were reduced to the neoclassical ion heat diffusivity level [6]. Boundary conditions on the separatrix for the bulk plasma parameters were set according to empirical relation $n_s = 0.3\cdot\langle n_e\rangle$ and approximation $T_s(eV) = (90\cdot P_{loss}(MW) / n_{s19})^{2/3}$ based on the B2-Eirine simulation results.

2. Estimation of plasma contamination by impurities on the limiter phase of discharge.

In the current ramp up phase of discharge before the x-point formation (when plasma current $I_p < 7.5$ MA) plasma column is bounded by the limiter. On this discharge stage the limiter sputtering is the main source of impurities in the plasma. At present, the question which material should be chosen for the ITER limiters is under discussions with possibility of using the limiter coating by tungsten in particular. In this section the results of modeling of the limiter stage of ITER discharges for the cases of beryllium and tungsten limiters are presented.

We modeled the current ramp up phase using parameters of the ITER scenario [7] for the plasma current interval $0.2 < I_p < 7.5$ MA. As at present there is no reference scenario for the rise of plasma density, we selected gas puffing as a main plasma fuelling method providing plasma average density of 0.5 of the Greenwald density limit. At smaller density boundary temperature is higher (what increases sputtering) and at higher density probability of disruption increases.

We suggested that the main impurity production mechanisms are the limiter sputtering by bulk D/T ions escaping the plasma and self-sputtering by ions of limiter material with different charge on the plasma periphery. Bombardment of the limiter by ions accelerated in the limiter sheath potential results in the limiter surface erosion. To estimate the maximum effect, we did not take into account sheath potential reduction due to the secondary electron emission and used the expression: $e\varphi_L / T_e= 0.5\cdot\ln\{ m_i / [2\pi m_e (1+T_i/T_e)] \}$, which gives for D/T plasma with $T_i = T_e$, $e\varphi_L \approx 3\, T_e$. We assumed that ions sputtered the limiter had the energy $E \sim k\cdot e\cdot\varphi_L \sim 3\cdot T_e\cdot k$ (k is the ion charge).

For estimation of the electron temperature at the plasma boundary we used the simplest assumptions: $T_{es} = T_{is} = T_s$, that there are no sources and sinks (such as ionization, recombination, heating and radiation) in the SOL, and that power flux through the separatrix comes to the limiter with the particle flow along the field lines. In this case the power flux to the limiter is equal to $P_{loss} \sim 5 \cdot \Gamma_s \cdot T_s$, where Γ_s is the particle flux through the separatrix which in steady state conditions is equal to the particle flux to the limiter. This gives $T_s = P_{loss} / 5 \cdot \Gamma_s$. P_{loss} and Γ_s were simulated in the bulk plasma model by ASTRA code. To estimate the maximum effect we neglected possible reduction of the edge plasma temperature due to increase of the particle recycling on the limiter. The empirical relation $n_s = 0.3 \langle n_e \rangle$ have been used for the description of the boundary electron density.

Fig.1 demonstrates results of the modeling of current ramp-up phase for the basic inductive ITER scenario (without auxiliary plasma heating in this discharge stage) with beryllium coating of the limiters.

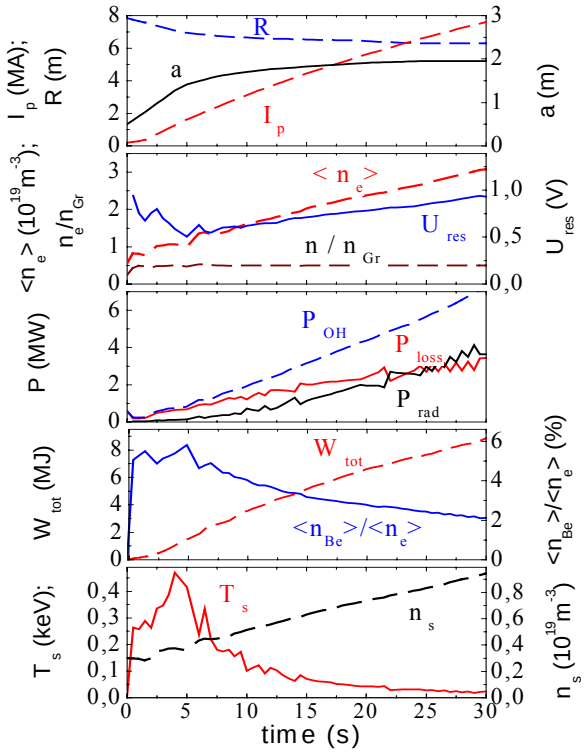

FIG.1 Evolution of parameters during plasma current ramp-up stage of the inductive ITER scenario with the beryllium limiter.

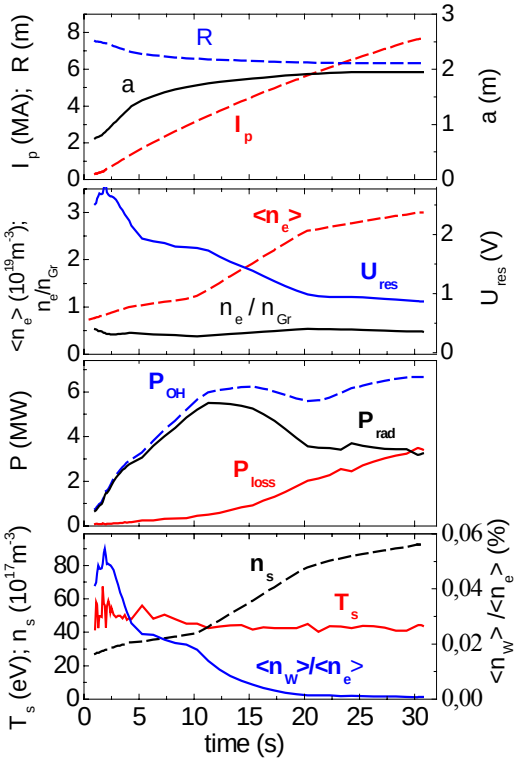

FIG. 2 Evolution of parameters during plasma current ramp-up stage of the inductive ITER scenario with the tungsten limiter.

Plasma column was formed initially near the outer limiter, which fixed plasma size. Then simultaneously with rise of the current plasma column was shifted to the vacuum vessel center what resulted in increase of the minor radius. Separatrix configuration in this scenario appeared approximately at 30th second at plasma current of 7.5 MA.

In this case the change of resistive voltage was small and Ohmic power increased together with I_p to the value ~ 6 MW in the end of this stage. Initially plasma radiation was small and power flux through the separatrix P_{loss} was close to the Ohmic power. Because of small density in the discharge beginning boundary temperature was high enough (~ 300-400 eV) what results in relatively strong limiter sputtering and enhanced beryllium concentration in plasma (~5-6 %).

With rise of the plasma density the radiated power increased and power flux through the separatrix was stabilized on the level of 2-3 MW, in spite of P_{OH} rise. In this time boundary temperature and limiter sputtering decreased and to the time of separatrix formation beryllium contamination decreased to the level of ~ 2 % (the level characteristic to the reference regime [4]). To the end of this discharge stage about half of the total power was re-radiated. Boundary temperature reached its maximum in the time 3-5 s.

Fig.2 demonstrates dynamics of discharge characteristics for the case of the tungsten limiter. Simulations show that in the very beginning of the discharge (at small plasma density), when conditions for keeping the high boundary temperature existed, strong enough limiter sputtering was observed and tungsten contamination increased up to ~ 0.05 %. This on the one hand increased the loop voltage, the volt-second consumption and value of Ohmic power, which was in the beginning of discharge of about 2-3 times higher than in discharge with the beryllium limiter. On the other hand, enhanced radiation helped to re-radiate almost all injected in discharge power, then the power flux through the separatrix was small and after some oscillations peripheral temperature was stabilized on the relatively small level of ~ 40-50 eV when limiter sputtering is not too intensive. This effect corresponds to appearance of the negative feedback. Increase of edge temperature gives rise of impurity fluxes and corresponding increase of radiation. This reduces the temperature. On the contrary, at decrease of the temperature impurity fluxes and radiation decreases and temperature starts to rise.

Together with rise of the plasma density the tungsten contamination decreased what resulted in decrease of the loop voltage and plasma radiation. To the moment of the separatrix formation the main discharge parameters reached the same level as in the discharge with the beryllium limiter.

Simulations showed that in this case the most critical was the discharge initiation stage before 4-5 sec as in the previous case. We do not model stages of discharge breakdown and discharge formation with unclosed magnetic surfaces. Simulation was started from the current ~ 200 kA when plasma column with closed magnetic surfaces was formed at small tungsten content ~ 0.01-0.03 %. To the moment of 2-3 sec tungsten content increased to the level of ~ 0.05 % and then dropped. However at higher initial tungsten content (if for the moment 2-3 s it reached level higher than ~ 0.055 %) supercooling instability started. It started at radial position where T_e was equal to 200-300 eV. In this temperature range the radiation increases with a drop of temperature and positive feedback is appeared. Effect increased because in this region plasma current started to decrease, what resulted in decrease of Ohmic power and further cooling of the plasma. It can result in the radiative collapse and disruption. So this discharge stage requires further investigation and optimization.

3. Impurity behaviour on the current flat-top stage of discharge.

At present, there is no systematically tested model of the impurity transport. Experiments on different tokamaks often show contradictory results. So, we consider cases with different contributions of the neoclassical and anomalous impurity transport on the example of different discharge scenarios. As the neoclassical contribution increases with the charge number one can expect that neoclassical transport should dominate in ELMy H-mode scenario for high-Z impurities and in ITB regions of enhanced confinement regimes for any impurities. Modelling [1,8] performed for tungsten impurity in the ITER inductive ELMy H-mode scenario 2 [4] in

assumption of the neoclassical transport only, demonstrated effective screening of the plasma core from this impurity. In this case impurity was concentrated near the plasma boundary.

3.1 ITER steady-state scenario.

Neoclassical effects can give high contribution also in the steady-state ITER scenarios with a broad zone of a reversed shear (RS) in the plasma core. According to experiments [9,10], inside the ITB region the impurity transport was found to be close to the neoclassical theory predictions. Simulated radial profiles of plasma parameters for the possible ITER steady-state scenario with I_p = 9 MA and average plasma density $6.8 \cdot 10^{19} m^{-3}$ are shown in Fig.3. In the RS region anomalous transport coefficient D_A decreases to zero. Simulation show that in this case

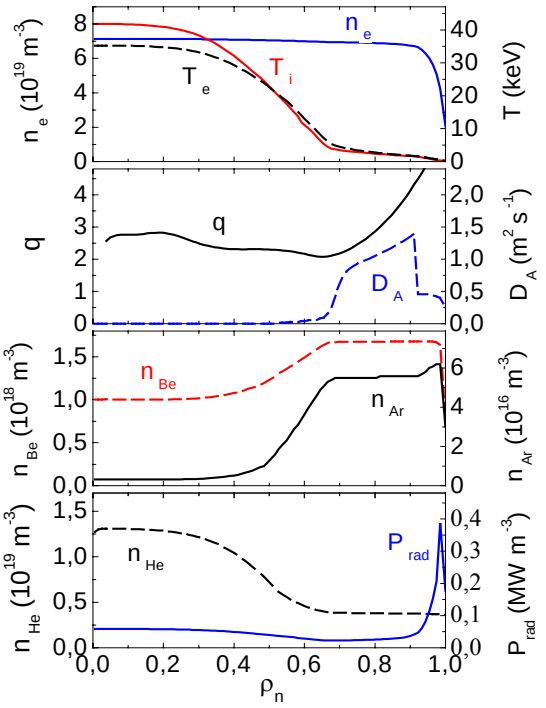

FIG. 3 Radial profiles of discharge parameters for the ITER steady-state RS scenario.

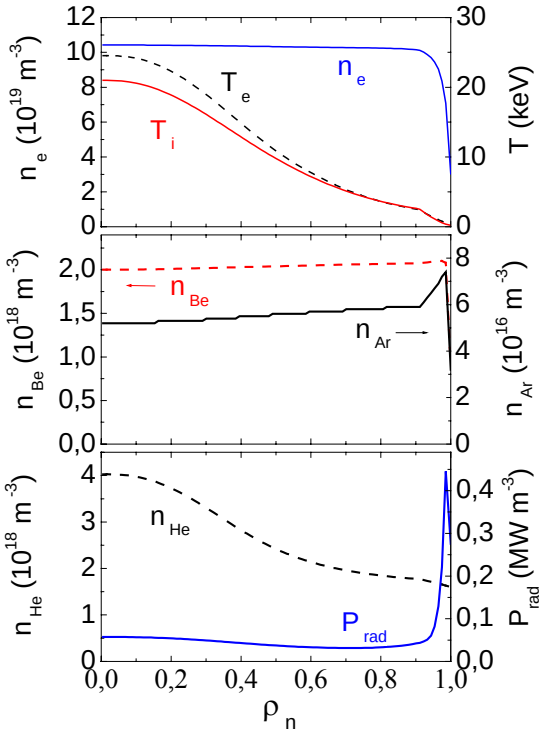

FIG. 4 Radial profiles of plasma parameters for the ITER inductive scenario.

argon ions escape the plasma core with the RS region and concentrate in the plasma periphery where the anomalous diffusion effectively mixes impurities and flattens their density. Beryllium density decreases towards the plasma center more slow than the argon one. Helium concentrates in the plasma core because its source is peaked. Because of small impurity content in the plasma core confinement in this region is rather good and helium accumulation in the plasma core helps to prevent plasma overheating. To obtain desirable helium content for fusion power stabilization, we decreased helium pumping speed on the plasma boundary in this case to the value corresponding to the relation $\tau_{He} / \tau_E \sim 10$. Due to the good CD efficiency CD power for driving current of I_p= 9 MA was not too high ~ 57 MW (30MW of NBI and 27 MW of off-axis RF) and Q = 5 we obtained at P_{fus} =285 MW. Plasma radiation in this case rises towards the plasma periphery.

3.2 ITER reference inductive scenario.

Fig.4 demonstrates profiles of the plasma parameters for the reference ITER inductive scenario 2 which is based on the ELMy H-mode regime with the fusion power P_{fus} ~ 400 MW, Q value ≥10, toroidal magnetic field B_o= 5.3 T, plasma current Ip = 15 MA and average electron density $<n_e>$ ~ $10.1 \cdot 10^{19} m^{-3}$ [4]. In this regime anomalous transport considerably exceeds the neoclassical one. In spite of this, in the absence of strong anomalous impurity pinch neoclassical contribution remains noticeable and prevents impurity accumulation in the plasma core.

In [11] influence of anomalous impurity pinch on impurity accumulation have been considered. According to these simulations, in the case when anomalous pinch is taken to be the same for all plasma components (this case is most close to the experimental findings) the enhanced impurity accumulation is absent. Impurity density profiles were similar to the bulk plasma density profile and profile of Z_{eff} remains flat when pinch velocity increases.

In all considered cases plasma radiation has the maximum near the plasma boundary (Figs.3.4). As it was pointed in [1,8] in this radiative layer P_{rad} exceeds approximately twice the value calculated in the coronal approach. This can be explained by the influence of charge exchange of impurity ions with hydrogen isotope neutrals fuelling the plasma. Such hollow profile of radiation is favorable for creating the re-radiating mantle at the edge.

The behaviour of impurities in considered scenario can be perturbed by MHD instabilities. The influence of sawteeth is insignificant because of the flat impurity concentration profiles in the central region. The ELM instability results in periodic oscillations of plasma parameters near the edge and can redistribute impurities. As simulations show [1,8] in ~ 100 ms after the ELM all perturbations vanish and all radial distributions return to their unperturbed form. Characteristic time of ∇p restoration determined possible ELMs frequency, which was established on the level of about 10 Hz or somewhat higher. In simulations ELMs did not perturb impurity density in the plasma core affecting the periphery region only. During the ELM impurity concentration decreases and after the ELM we see some concentration of impurity in the region of the edge transport barrier. If time interval between ELMs was longer than 100ms impurity contamination was restored. If this interval was shorter, the impurity contamination had no time for restoration. As a result one could see some decrease of impurity concentration in the core despite of the fixed impurity influx from the boundary.

4. Dependence of plasma parameters on impurity concentration. Critical impurity concentrations.

Increase of impurity concentration in plasma results in fuel dilution and rise of plasma radiation. This decreases fusion reactivity and cools the plasma. Decrease of the power flux through the separatrix to the level smaller than H-L-mode threshold power can induce transition to L-mode with deterioration of confinement and further plasma cooling. At high impurity concentration the discharge parameters (P_{fus} and Q) are moved out from the operational window of the basic regimes. One can keep fusion reactivity and power flux through the separatrix by increasing the auxiliary heating power. However, this decreases Q value. Besides, the level of auxiliary power is limited. Therefore, available level of auxiliary power and accessible Q value determine the value of critical impurity concentration for some scenario. Characteristic values of the critical concentrations of different impurities for ITER can be found, for example, for the reference inductive scenario with the fusion power $P_{fus} \approx 400$ MW.

Fig.5 demonstrates results of such calculations. Change of plasma radiation versus relative impurity concentrations is shown in the lower figure. Upper figure shows auxiliary heating powers necessary for keeping reference fusion power $P_{fus} \approx 400$ MW. Corresponding Q values, power through the separatrix P_{loss} and relation of this power to the H-L transition threshold power are presented in the middle part of the figure. NBI power has been used as auxiliary heating power (using of other kinds of heating power at good electron-ion energy coupling gives similar values of parameters). Results for different impurities expected in ITER plasma are presented. Black dashed lines which characterize level of critical concentrations are plotted for the maximum available P_{aux} = 130 MW i.e. Q ≈ 3. Results for other P_{aux} limits can be obtained from this figure also. In the simulations the variation of different impurity concentrations was studied at the fixed helium pumping providing τ_{He}/τ_E =3. While variation of the He concentration was produced in the modeling by changing its pumping speed in the absence of other impurities.

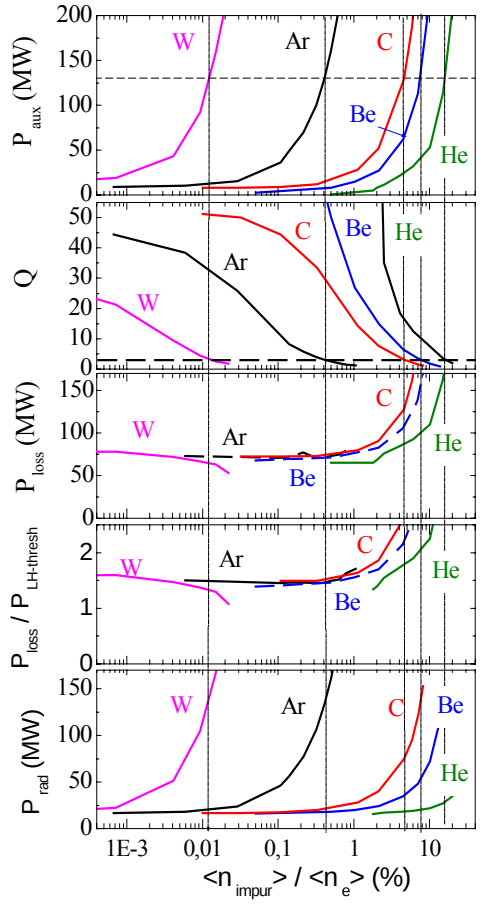

FIG.5 Change of plasma parameters versus impurities concentrations.

One can see that processes determining maximum concentrations of low-Z and high-Z impurities are slightly different. For example, in the case of tungsten the main effect is connected with the increase of radiation (influence of fuel dilution is smaller). In spite of the rise of auxiliary power, flux through the separatrix decreases and a danger of the reversed H-L transition increases together with achieving the limit in P_{aux}.

In the case of low-Z impurities (C, Be, He) fuel dilution is the dominant process. Radiation losses increase slower than necessary P_{aux}. That is why P_{loss} increases and danger of reversed H-L transition does not exist. In this case the level of critical concentrations is determined by the value of the available auxiliary power and Q value.

For an impurity with intermediate charge number as argon, increasing the level of P_{aux} is completely compensated by increasing the radiation power P_{rad} and change of P_{loss} is absent.

As a result, we obtain for critical concentrations of impurities the values: for tungsten ~ 0.013 %, for argon ~ 0.4 %, for carbon ~ 5 %, for beryllium ~ 8 % and for helium ~ 16 %.

Simulations show that in the absence of all impurities except for helium and at good He pumping (corresponding to $\tau_\alpha/\tau_E < 2$ or He concentration smaller than 1-2 %) one can achieve in ITER Q values higher than 100 in the inductive scenario with HH(y2) =1.

Saturation of Q values on the level ~ 50 even at a small content of other impurities is connected with helium contamination determined by the fixed pumping speed (corresponding to $\tau_{He} / \tau_E = 3$).

5. Conclusions

Results of the modelling indicate that:

--- In all considered scenarios excessive impurity accumulation in the plasma core is absent.

--- Plasma radiation considerably increases to the plasma column periphery. This assists to formation of the re-radiating layer (radiation mantle) near the plasma boundary.

--- Modelling of the limiter discharge stage showed that on this stage considerable re-radiation of power is possible. This can decrease heat loads on the limiter and its sputtering.

In the case of beryllium limiter up to half of the injected in plasma power can be radiated. In the case of the tungsten limiter in the start of discharge almost all injected power is radiated resulting in stabilization of the boundary temperature and limiter sputtering.

--- However, these conditions depend strongly on impurity contamination in the initial discharge stage (at t ~ 1-2 sec). If for tungsten this level exceeds ~ 0.055 % radiative collapse of plasma column is observed.

--- Simulations showed that the very beginning of discharge (during $t < 5s$ when maximum contamination of plasma column by impurities is observed) is the most critical stage in view of the radiative collapse possibility. So, more comprehensive investigations of this stage and its optimization are required.

--- To the time of the separatrix formation impurity contamination of plasma decreases to the acceptable level and father plasma heating can be started and burning stage of discharge can be initiated.

--- Critical impurity concentrations of different impurities are calculated for the flat-top stage of the basic ITER scenario.

--- It should be noticed that simulations have not demonstrated serious reasons against application of high-Z materials (for example tungsten) for the plasma facing components in ITER, if loss power is controlled by the radiation mantle.

Apparently, realization of such re-radiating layer for the control of loss power can help to improve the discharge performance in the present tokamak experiments, where high-Z materials are used.

The work is supported by Nuclear Science and Technology Department of Rosatom RF and grant SS-1880.206.2.

References

1. Leonov V.M., Zhogolev V.E., Plasma Phys. Control. Fusion **47** (2005), 903
2. Pereverzev G.V., Yushmanov P.N., Preprint IPP 5/98, Garching 2002
3. Houlberg W.A. et al, Phys. Plasmas **4** (1997), 3230
4. Green B.J. for the ITER Teams, Plasma Phys. Control. Fusion **45** (2003), 687
5. ITER Physics Basis, Nucl. Fusion **39 (**1999), 2175
6. Chang C.S, Hinton F.L, Phys.Fluids **29** (1986) 3314
7. Lukash V., Gribov Yu. et al. , Plasma D&O v.13, N2 (2005) 143
8. Zhogolev V., Leonov V., 2005 32th EPS (Tarragona, Spain) P2.119
9. Chen H. et al., Nucl.Fusion **41** (2001) 31
10. Dux R. et al., 2002 Proc.28th EPS (Madeira, Portugal) P2.007
11. Leonov V., Zhogolev V., 2006 33th EPS (Roma, Italy) P1.129